Experimental Demonstration of Super-Mode Converters in a Multi-Layer InP Photonic Integrated Circuit

J.Ø. Kjellman, S. Cardarelli, R. Stabile and K.A. Williams

Institute for Photonic Integration, Eindhoven University of Technology, Eindhoven, The Netherlands

A multi-layer photonic integrated circuit is created with fundamental mode to super-mode conversion building blocks. Excitation of super-modes are demonstrated in tapered dual layer, dual width waveguides which are expected to enable dispersion engineered integrated photonics.

Introduction

Multi-layer photonic integrated circuits offer the prospect of both enhanced connectivity, and new component-level functionality. Epitaxially-grown, vertically-stacked waveguide cores also enable high-precision and close-proximity layers for advanced mode engineering.

Dual layer, dual width waveguides have been proposed to enable a new class of dispersive InP integrated photonic circuits [1]. These waveguides are designed to exhibit giant group velocity dispersion (GVD), which is a phenomena of enhanced dispersion around a geometrically determined resonance wavelength [2]. The waveguide dispersion of the dual layer waveguides is predicted to be an order of magnitude larger than the material dispersion [1]. Furthermore, the waveguides offer the ability to engineer both the magnitude and sign of the dispersion. These dispersive waveguides are also designed to be fully backwards compatible with existing single-layer active and passive components in our institutes InP photonic integration platform [3]. These qualities should enable a wide range of dispersive circuit to be realized as single chip systems. Examples of such potential circuits include chirped pulse amplifiers [4], all optical oscilloscopes [5], and radio beam steering devices [6].

Here we report on the experimental demonstration of a new class of super-mode converters suitable to excite giant dispersion waveguides. We report on the design and fabrication of the super-mode converters, and evaluate them across a wavelength range from 1500 nm to 1600 nm by imaging of the optical field at the output facet.

Mode converters

The dual layer, dual width waveguides consists of two InGaAsP cores of different composition (Q1.25 and Q1.40) and different widths which are separated by an InP spacer. These support symmetric and antisymmetric super-modes which exhibit giant group velocity dispersion [1]. To excite these super-modes, mode converters are designed which consists of a single core input waveguide leading to a dual core butt-joint followed by a tapering of the top core width as illustrated in fig. 1. Given an excitation of the single core waveguide's fundamental mode at the input we expect the dual layer waveguide's super-mode to be excited at the output. These super-modes are either symmetric or antisymmetric in phase and are selected for by the width of the top core at the single to dual core butt joint. The design resonance wavelength is 1600 nm, where the field is distributed between the upper and lower core either symmetric or

antisymmetric. It is at this wavelength the dispersion is strongest. Simulations with the Fimmwave mode solver from PhotonDesign gives a GVD of $64000\ \mathrm{ps\ (nm \cdot km)^{-1}}$ and $-86000\ \mathrm{ps\ (nm \cdot km)^{-1}}$ for the symmetric and antisymmetric modes, respectively.

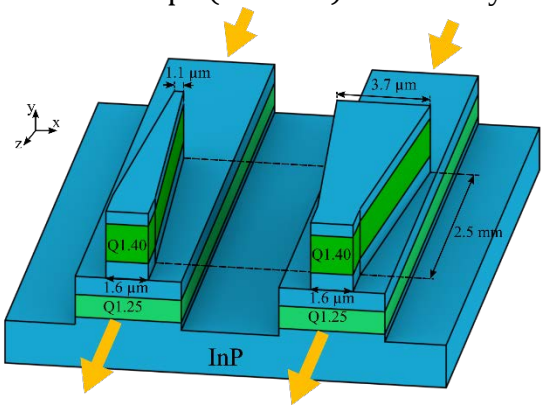

Figure 1: Mode converter designs (not to scale.) excitation of antisymmetric (left) and symmetric (right) super-modes. Layer thicknesses are, top to bottom, 650 nm, 1100 nm, 1000 nm, and 500 nm.

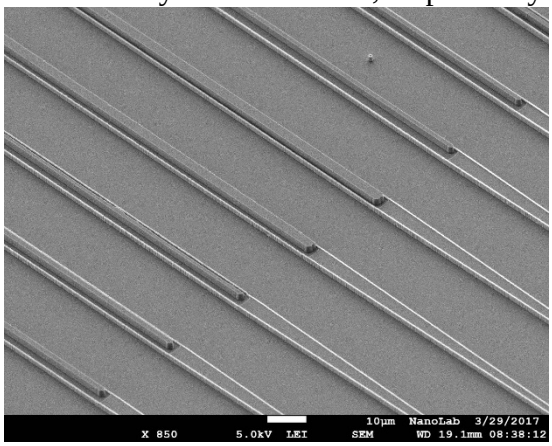

Figure 2: SEM image of array of mode converters of different geometries.

Results

Devices were fabricated in a process using contact photolithography and established InP etching processes [7]. Figure 2 shows an array of single layer to dual layer butt-joints for a set of mode converter designs. After fabrication, light is coupled into a single layer input waveguide from a tunable laser source using a lensed fiber and the optical intensity distribution at the cleaved output facet is imaged with a $50\times/0.8\mathrm{NA}$ microscope objective and a $f = 75$ cm lens, and captured with an infrared camera. The polarization is optimized for TE at the output and no polarization rotation is expected in the straight guides. The design geometry of the measured devices is indicated in fig. 1.

For the symmetric mode converter, clear evidence of super-mode excitation is obtained. Figure 3b shows the captured output intensity distribution at a wavelength of 1590 nm. Three lobes are clearly visible as expected when a super-mode has been excited indicating that this wavelength is near the resonance wavelength. Furthermore, looking at a set of measurements at three wavelengths in figs. 3a-c and comparing it with the simulated mode profiles in figs. 3d-f reveals qualitative agreement with the expected trend. At shorter wavelengths power is confined in the lower core while at longer wavelengths it transitions to the upper core. However, the simulations are for the nominal design and have a resonance wavelength of 1517 nm indicating that there is around 70 nm red-shift of the super-mode resonance. We attribute this to variations in layer thickness, layer composition and waveguide dimensions. It should be possible to improve this by optimizing the fabrication process.

Figure 5 shows the captured intensity profiles averaged along the x-axis and plotted against wavelength. This figure confirms how the power is transferred from the lower waveguide to the upper waveguide. This in turn, indicates the successful excitation of the symmetric super-mode over a large bandwidth range. However, we also observe a break in this trend between approximately 1570 nm and 1590 nm.

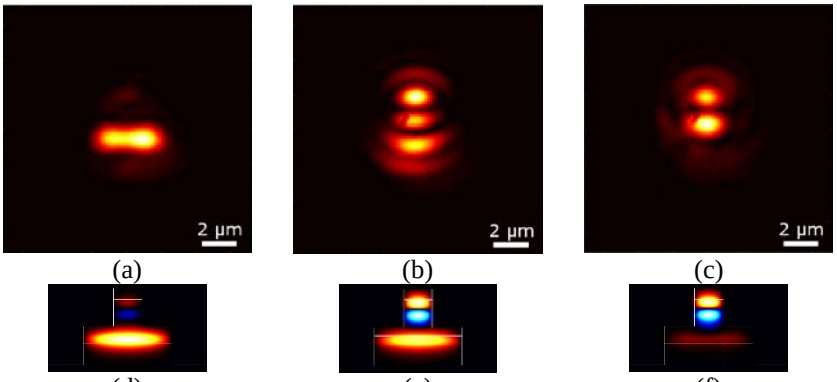

Figure 3: Captured images of optical field distribution at output of symmetric mode converter for wavelengths of (a) 1530 nm, (b) 1590 nm, and (c) 1600 nm. Simulated mode profiles (real E-field) for nominal symmetric mode converter design at wavelengths (d) 1492 nm, (e) 1517 nm, and (f) 1542 nm.

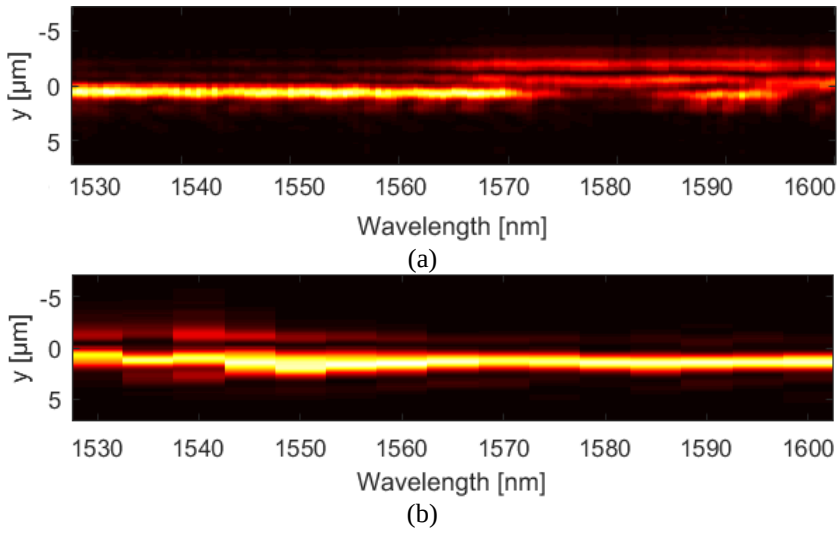

Figure 5: Captured optical intensity distribution averaged along x-axis and plotted against wavelength for (a) symmetric mode converter, and (b) antisymmetric mode converter.

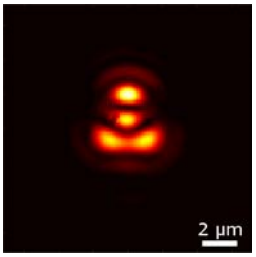

Figure 4: Captured optical intensity distribution of symmetric mode converter at 1570 nm wavelength.

Figure 5 shows the captured output intensity of the symmetric mode converter at a wavelength of 1570 nm. This figure shows a super-mode similar to the expected one in figs. 3b and 3e. Unlike the expected super-mode though, the captured one shows at this wavelength a split lower lobe. We attribute this to a super-mode composed of the first higher order mode in the lower core instead of the desired fundamental mode. This observation suggests that mode purity at the input is of high importance.

For the antisymmetric mode converter there is also suggestive evidence of super-mode excitation, but due to the resolution of the system, the results are less conclusive. Since, in this case, the lower core's lobe is in phase with the lower lobe of the upper core they cannot be readily resolved by a conventional free-space optical system due to the diffraction limit. However, fig. 6b, which shows the output intensity distribution at 1545 nm, corresponds qualitatively to what can be expected in a diffraction limited system. The upper lobe of the top core is clearly resolved indicating that it is 180° out of phase with the lower lobe. The lower lobe of the captured symmetric intensity profiles is believed to be composed of both the fundamental mode of the lower core and

the lower lobe of the first higher order mode of the upper waveguide. This is supported by the size and shape of the lobe, and by comparison with fig. 6c which shows how power is confined to the lower cores fundamental mode at a wavelength of 1600 nm.

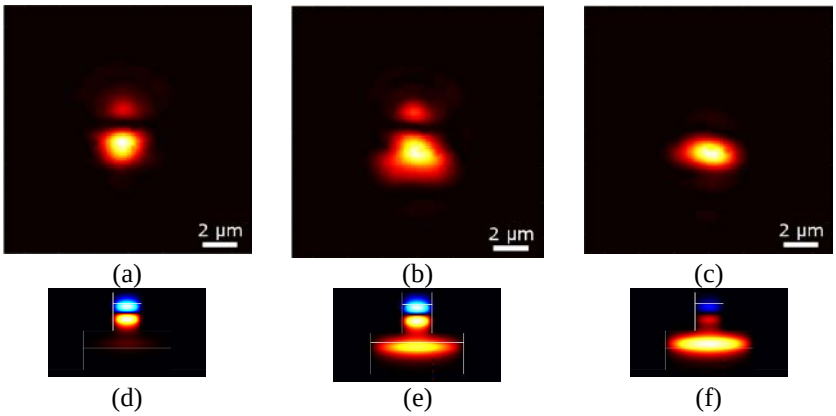

Figure 6: Captured images of optical field distribution at output of the antisymmetric mode converter for wavelengths (a) 1530 nm, (b) 1545 nm, and (c) 1600 nm. Simulated mode profiles (real E-field) for nominal antisymmetric mode converter design at wavelengths (d) 1492 nm, (e) 1517 nm, and (f) 1542 nm.

Comparing the captured output intensity in figs. 6a-c to the simulated mode profiles in figs. 6d-f does suggest qualitatively that the device follows the predicted trend at least for longer wavelengths. At shorter wavelengths, as seen in fig. 6a, significant power still remains in the lower core, but there is a shift towards the upper core. This is confirmed by plotting the average cross-section against wavelength as shown in fig. 5b. This plot suggests that the power shifts from a distribution between the two cores at short wavelengths to being confined in the lower core at long wavelengths. This is consistent with the excitation of an antisymmetric super-mode.

Conclusion

Experimental evidence of conversion from the fundamental mode of a conventional single core waveguide into the super-modes of dual layer, dual width waveguides has been obtained by imaging of the intensity distribution at the super-mode converter outputs. This represents an important step in bringing dispersion engineering and all-integrated ultrafast optical pulse processing to integrated photonic circuits.

References

[1] J. Ø. Kjellman, R. Stabile, and K. A. Williams, “Broadband giant group velocity dispersion in asymmetric InP dual layer, dual width waveguides,” J. Lightwave Technol., 35 (17), 2017.
[2] U. Peschel, T. Peschel, and F. Lederer, “A compact device for highly efficient dispersion compensation in fiber transmission,” Appl. Phys. Lett., 67 (15), 1995.
[3] M. Smit et al., “An introduction to InP-based generic integration technology,” Semicond. Sci. Technol., 29 (8), 2014.
[4] P. Maine, D. Strickland, P. Bado, M. Pessot, and G. Mourou, “Generation of ultrahigh peak power pulses by chirped pulse amplification,” IEEE J. Quantum Electron., 24 (2), 1988.
[5] M. A. Foster, R. Salem, D. F. Geraghty, A. C. TurnerFoster, M. Lipson, and A. L. Gaeta, “Silicon-chip-based ultrafast optical oscilloscope,” Nature, 456 (7218), 2008.
[6] R. Soref., “Optical dispersion technique for time-delay beam steering,” Appl. Opt., 31 (35), 1992.
[7] J. Ø. Kjellman, R. Stabile, and K. A. Williams, “Fabrication of dual layer, dual width waveguides for dispersion engineered indium phosphide based photonic circuits,” IEEE Photonics Conference 2017